WATER DESORPTION ISOTHERMS OF CEMENT MORTAR WITH FLY ASH

Xu Aimin
Division of Building Materials
Chalmers University of Technology
Göteborg, Sweden

ABSTRACT

This investigation shows the water sorption isotherms of ordinary Portland cement mortar incorporated with pulverized fly ash (PFA). The variation in the mixture proportions are: PFA to binder ratio from 0 to 0.60, water to binder ratio from 0.36 to 0.60, and sand to binder ratio from 1 to 4.

Based on the systematic experimental design, the analysis quantitatively shows the relations between the mixture proportions and the properties of mortar.

It is shown here that the moisture content in mortar mainly depends on the amount of cementitious materials in the mortar. The sorption isotherm changes with the addition of fly ash and the variation in water to binder ratio. The carbonation can greatly influence the desorption isotherm and the pore size distribution.

This paper shows the pore size distribution of the mortar calculated according to the desorption isotherm by taking the adsorbed water film into account.

Keywords: Fly ash, Desorption, Isotherm, Carbonation, Pore size distribution.

1. INTRODUCTION

The water sorption isotherm is closely related to the specific surface area of cement paste and the pore structure in concrete and mainly where the small capillary pores are concerned.

The use of fly ash as a cementitous material in concrete has increased since the 1960's, and extensive research work has been

carried out on the effect of fly ash on the strength of concrete. It has been noticed that concrete to which fly ash has been added is more sensitive to the environmental moisture condition. However, systematic studies on the behaviour of cement - fly ash mortar in different unsaturated moisture conditions are scarce.

The effect of fly ash on the pore structure of the cement matrix is mainly because of the hydration of the fly ash. However the reaction consumes the cement hydration products, e.g. $Ca(OH)_2$ thus lowers the resistance of concrete to carbonation which in turn changes the pore structure and affects the sorption behaviour.

This paper presents the test results of sorption isotherms of cement mortar with fly ash. The main influencing factors studied are the fly ash content, the water to binder ratio, sand content, and carbonation.

The calculation of pore size distribution is affected by the simultaneous evaporation of water from the core and from the inner surface of the capillary. The paper shows the pore size distribution calculated from the desorption isotherm.

The results of the calculation on the basis of the isotherms show that the pore size distribution of the mortar is significantly affected by the addition of fly ash, and by carbonation.

2. EXPERIMENTAL

2.1 Materials

A Swedish fly ash, which is commercially available and meets the requirements of ASTM C 618, was tested. Its composition and

Table 1. Composition and property of the materials.

Fly Ash		Cement	
SiO_2	48.6 %	C_2S	64.0 %
Al_2O_3	22.0 %	C_3S	13.0 %
CaO	10.0 %	C_3A	8.0 %
Fe_2O	11.0 %	C_4AF	10.0 %
K_2O	2.0 %	MgO_3	4.0 %
Na_2O	0.2 %	SO_3	0.8 %
Ignition loss	2.8 %		
Water requirement	92.0 %		
Sp.surface(Blain)	365 m^2/kg		337 m^2/kg
Sp.gravity	2.334		3.150

physical properties are shown in Table 1. Ordinary Portland cement and standard quartz sand were used.

2.2 Influencing Factors

The sorption isotherms of a porous material are a reflection of its pore structure. The pore system is the space formerly occupied by the mixing water and entrained air. The inner surface of hardened cement paste, which is in contact with the moisture, is formed by the growth of CSH gel in the pores. Therefore the factors that effect the process of hydration and the pore structure are studied, i.e.

F/(C+F), the fraction of cement replaced by fly ash,
W/(C+F), water to binder ratio,
S/(C+F), sand to binder ratio,
$[CO_2]$, in percent by volume, the concentration of CO_2 in the accelerated carbonation process.

2.3 Specimen Preparation

Two series of mortar specimens were made.

1.The mortar with variation in F/(C+F) from 0 to 0.55, W/(C+F) from 0.45 to 0.60, and S/(C+F) from 1 to 4.

2.The mortar with variation in F/(C+F) from 0 to 0.60, and W/(C+F) from 0.36 to 0.57. S/(C+F) is kept at 2.5. The specimens were subjected to different concentrations of CO_2 at 76% relative humidity.

The orthogonal design plan $L_{16}(4^5)$ is used in the mixture design for the specimens in Series 1. The 16 different mixture proportions in Series 1 are expected to show the general dependence of the properties of the mixes on each factor. The mixture proportions are shown in Fig.1 together with the experimental data.

The mixtures for Series 2 are proportioned according to the second order surface fitting plan [5] in order to estimate nonlinear dependences.

40 × 40 × 160 mm prisms were made. They were demoulded 24 hours after casting. The Series 1 specimens were subjected to standard cure, i.e. water cured for 5 days followed by conditioned air cure at 20 °C and 50% relative humidity. The specimens Series 2-I and 2-II were only water cured, and Series 2-III was standard cured.

The 90 day mortar prisms were sawn into slices of a thickness of about 2.5 mm for testing the sorption isotherms.

2.4 Measurement of Desorption Isotherms

The water saturated specimen slices were placed in desiccators (size 21 × 17 × 12 cm) where the relative humidities (RH) were maintained by salt saturated water solutions, c.f. [1]. The time needed for establishing the constant RH in the desiccators are 6 hrs to 1 day depending on the salt and the desired RH [9]. The tightness of the desiccator was tested by placing a cup of $Ba(OH)_2$ in it which showed that the $BaCO_3$ precipitate occurred only when the desiccator was open. Thus the risk of the mortar being carbonated is limited since the volume of the desiccator is small and the times of weighing are limited. The specimens were weighed weekly on an analytical balance with an accuracy of 0.0001 gram.

2.5 Carbonation Process

Pure CO_2 gas was mixed with air according to the desired volume proportions. The mixed air was passed through a NaCl saturated solution which kept the relative humidity at 76%, and was led into the desiccator where specimens were stored. The concentrations of CO_2 are 0.04%, 5%, 13%, 20% and 25%.

3. RESULTS AND DISCUSSIONS

3.1 Desorption Isotherms

The desorption or drying of the hardened cement mortar is a diffusion controlled process. The moisture equilibrium state is established after about 2 months for the specimens at a relative humidity (RH) higher than 40%. However, about 70% of the total moisture loss occurred during the first week.

The desorption isotherm, i.e. equilibrium moisture content at different relative humidities at a constant temperature, varies with the change in the mixture proportion. Fig.1 shows the desorption isotherms in Series 1 presented as the amount of water per unit volume of specimen. In accordance with the principle of analysis of variables [5], the mean value of the data at each factor level is calculated and the analyzed isotherm curves are shown in Fig.2.

It can be seen that the increase in the fly ash content results in more moisture loss from the mortar at high RH, e.g. RH > 85% and less moisture content at low RH. However, the effect is the opposite when the fly ash content is lower than 20%. The moisture content at RH > 97% increases with F/(C+F), Fig.2a.

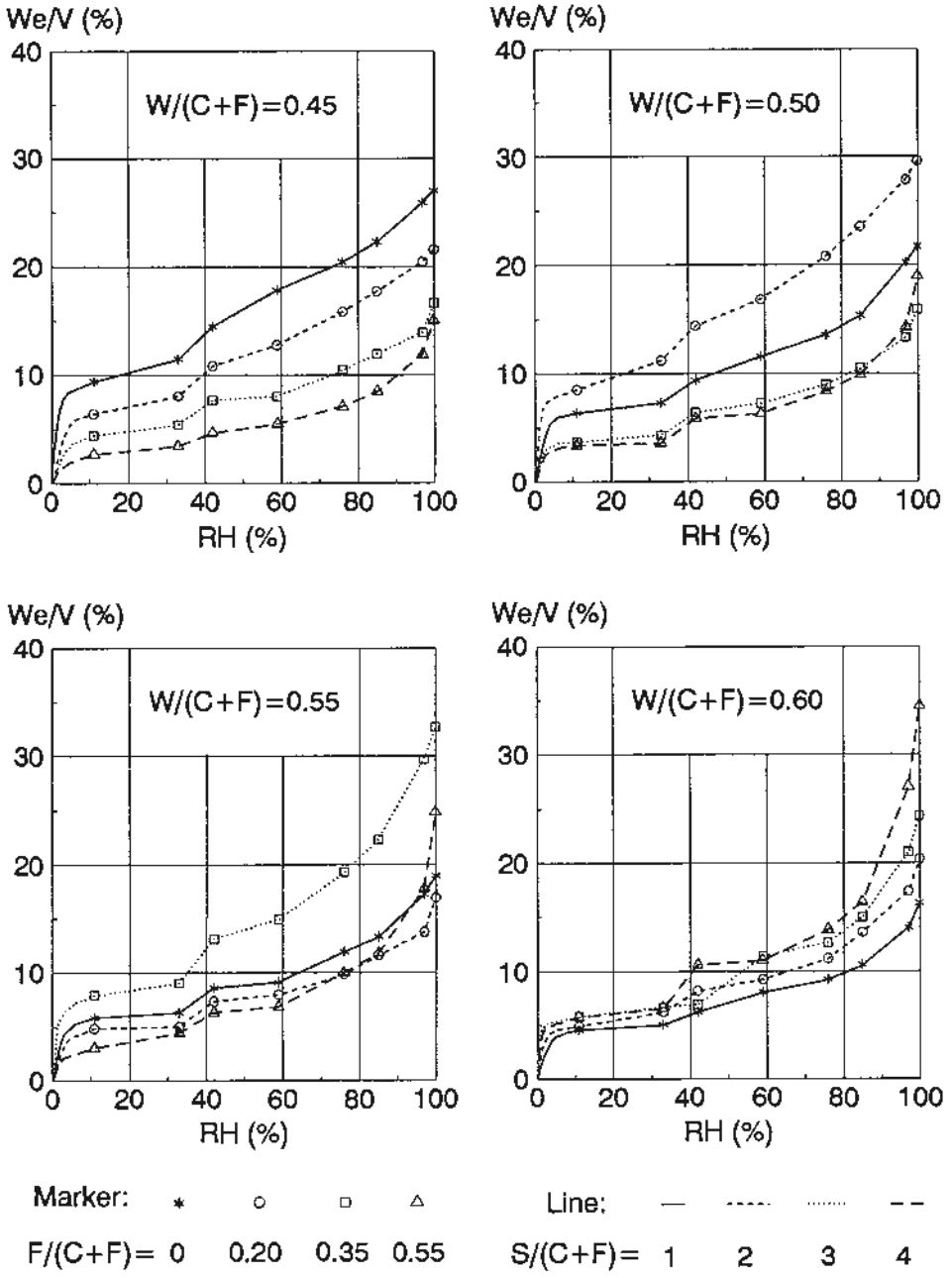

Fig.1 The desorption isotherms of cement mortar with F/(C+F)=0 ~0.60, W/(C+F)=0.45~0.60, and S/(C+F)=1~4.

The increase in water to binder ratio leads to higher porosity. The moisture content at RH > 90 % increases with W/(C+F). At RH about 90%, the difference in moisture content, for the specimens with different water to binder ratios is almost the same. At lower RH, the moisture content decreases with W/(C+F), Fig.2b.

The analysis of the effect of sand content is affected by the unit representing the moisture content. Because the porosity of the quartz sand is much lower than that of cement paste, the volumetric moisture content in mortar decreases with S/(C+F),

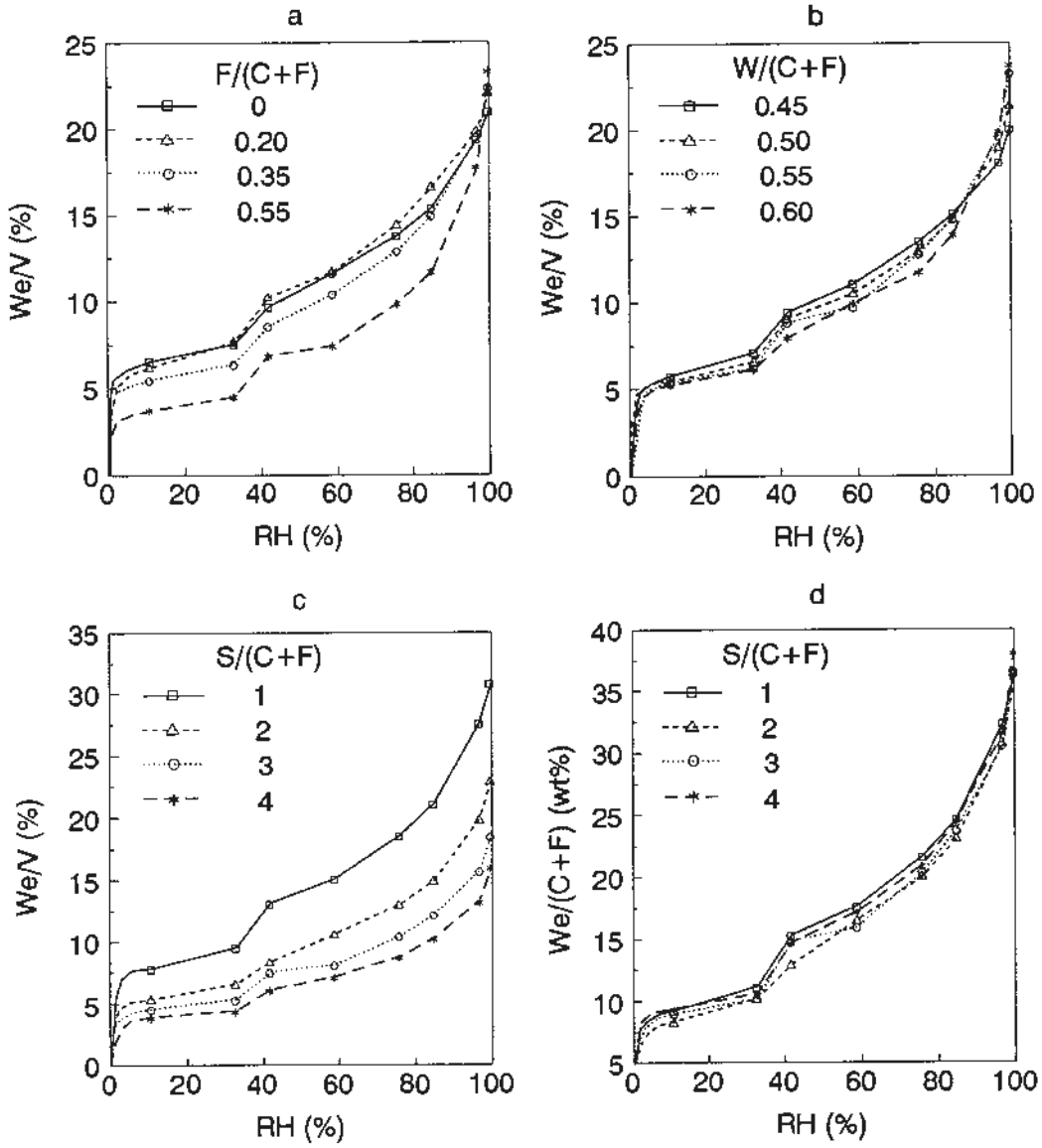

Fig.2 The analysis of factors affecting the isotherms.

Fig.2c. By rearranging the data as percentage of moisture per binder shows that sand content has little effect when S/(C+F)>2, Fig.2d.

Using the relation between meniscus curvature ($1/r_m$) and relative humidity, i.e. Kelvin's equation

$$\ln(p/p^\circ) = -2\gamma V/r_m RT \qquad (1)$$

where γ is the surface tension and V is the molecular volume of water, one finds that RH 90% corresponds to a pore radius 350 Å. Thus the increase in the moisture content at high RH, e.g. RH > 90% indicates a coarser pore system. In other words, both the high water to binder ratio and the high fraction of cement replacement with fly ash result in more capillary pores. In

contrast, the moisture held by the mortar at low RH is mainly due to the surface adsorption, and reflects the specific surface area in the solid porous material [3].

3.2 Specific Surface Area

The desorption isotherms are analyzed by applying the BET equation

$$\frac{X}{X_m} = \frac{ckp/p^\circ}{(1-kp/p^\circ)(1+(c-1)kp/p^\circ)} \qquad (2)$$

where c and k are constants, and X_m is the monolayer adsorption capacity, c.f. [2]. The specific surface area (S) is calculated by

$$S = \frac{Xm\ N\ \sigma}{M} \qquad (3)$$

where N, σ and M are Avogadro's constant, average area of water molecule (10.64 $Å^2$) and molecular weight of water (18 g/mol) respectively.

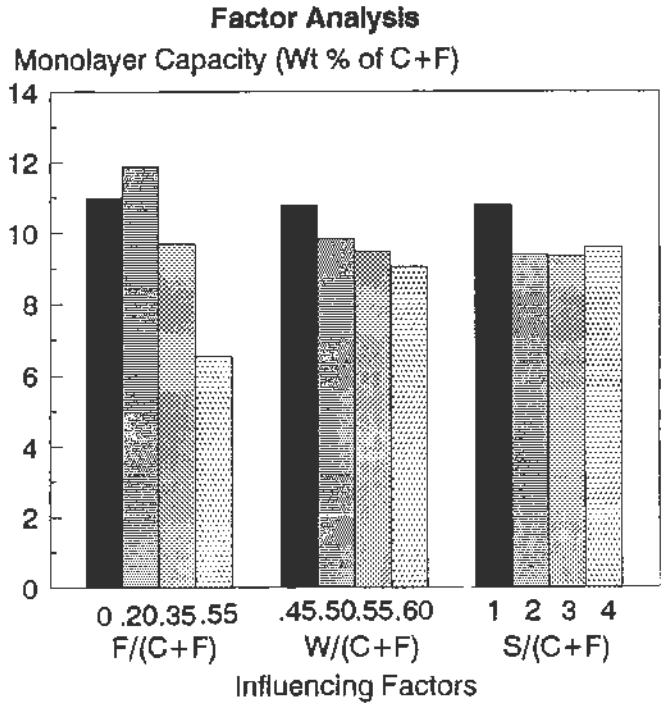

Fig.3 The effect of mix proportion on the monolayer capacity.

The results of the analysis (Fig.3) show that by replacing cement with fly ash, when F/(C+F) > 0.20, will result in a lower specific surface area. If only the cement is considered, the addition of fly ash leads to higher S. The contribution of fly ash to the specific surface area reaches its maximum value at F/(C+F) equal to about 0.20.

The increase in W/(C+F), on the other hand, leads to a decrease in S. The reduction in the specific surface area due to W/C+F can be explained by the existence of more crystal phases, e.g. $Ca(OH)_2$ in the pores. The over-saturation degree at an early stage of hydration decreases and the space for crystallizing increases with the increase in the water to cement ratio. The fly ash that replaces cement requires almost as much water for wetting its surface as cement needs. Thus the net water to cement ratio increases and a certain effect similar to increasing water cement ratio can be expected.

Comparing with Series 1, the desorption isotherms of Series 2 show less moisture loss at high RH, while the monolayer capacity is similar. The difference between the two series lies in the curing procedure. The existence of CO_2 in the climate room where Series 1 was cured could be one of the reasons for the difference in the isotherms as will be seen in the following results.

3.3 The Effect of Carbonation

The desorption isotherms of carbonated specimens (Series 2-II, and 2-III) are shown in Fig.4 comparing with the isotherms of the mortar without carbonation (Series 2-I). It is seen that the moisture loss becomes greater the higher relative humidities.

The total moisture content is lower especially in the case of

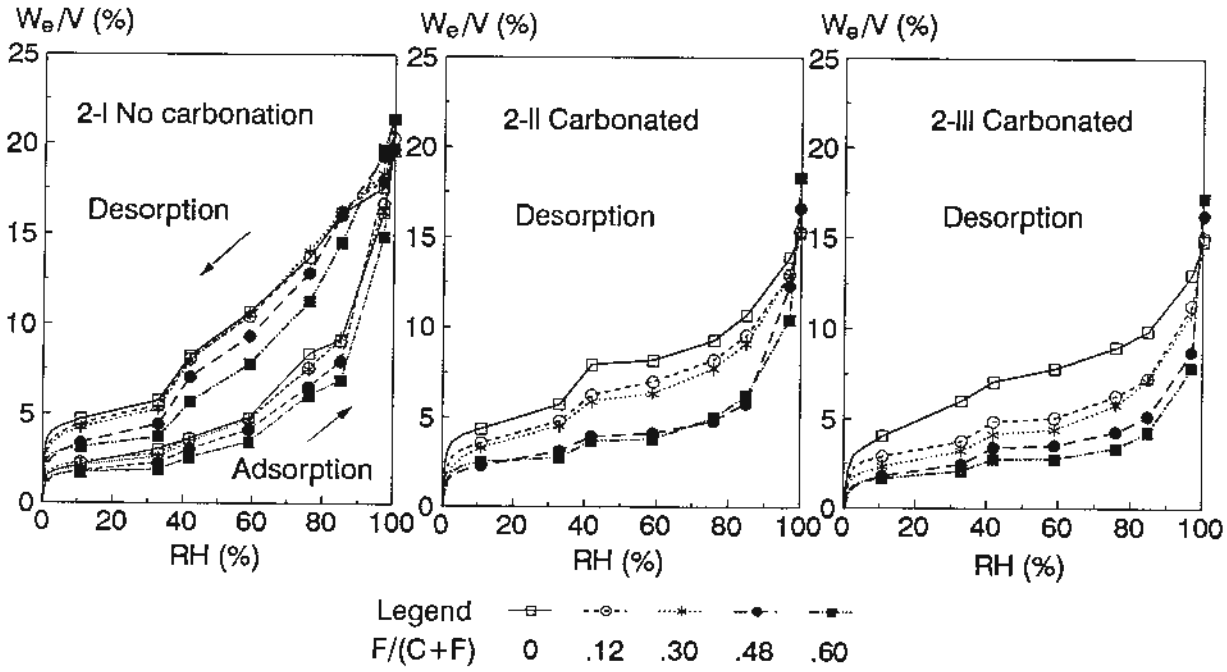

Fig.4 Sorption isotherms of the mortar with and without carbonation. The analysis of the effect of fly ash at W/(C+F)=0.4, S/(C+F)=2.5.

low fly ash content. The total pore volume decrease of the fully carbonated mortar was equal to about 0.03 to 0.06 g H_2O/cm^3, the lower value (0.03) corresponds to the mortar with F/(C+F)> 0.3. The increase in CO_2 concentration enhanced this effect. At RH 11%, moisture content decreased to 2/3 or 1/2 of that without carbonation, except for the specimens without fly ash which showed no practical difference for RH < 42%.

That is to say that the pores of the cement paste become coarser

after carbonation while the large capillary pores are partly filled by carbonates.

It is known that $CaCO_3$ has a higher specific molecular volume than $Ca(OH)_2$. Thus, a part of the pore volume is filled by the increase in solid volume due to carbonation, e.g. carbonation of $Ca(OH)_2$ to calcite results in a volume increase of about 0.044 cm^3/g $Ca(OH)_2$. The tested values are 0.06-0.12 cm^3/g C+F (Table 2). The total CaO in the cement and the fly ash is about 61% and

Table 2. The effect of carbonation on the characteristcs of the isotherm.

			Series 2-II						Series 3-III					
$\frac{F}{C+F}$	$\frac{W}{C+F}$	$[CO_2]$ (%)	Xm g/cm^3	K	W∞ g/cm^3	b	s	δV/(C+F) cm^3/g	Xm g/cm^3	K	W∞ g/cm^3	b	s	δV/(C+F) cm^3/g
.478	.527	25	.0201	.8465	.1855	4.33	2.19	.0751	.0158	.8545	.1792	6.09	2.02	.0863
.478	.527	.04	.0161	.8837	.1761	4.72	2.15	.0629	.0162	.8590	.1776	5.58	2.12	.0602
.478	.403	25	.0245	.7801	.1469	3.15	1.81	.0739	.0187	.8148	.1451	4.41	1.78	.0769
.478	.403	.04	.0191	.8533	.1560	3.94	1.77	.0585	.0192	.8257	.1495	4.22	1.74	.0696
.122	.527	25	.0354	.7401	.1578	2.26	1.65	.1169	.0249	.7937	.1531	3.10	1.82	.1255
.122	.527	.04	.0313	.8029	.1670	2.70	1.50	.0756	.0212	.8415	.1651	3.51	2.03	.0789
.122	.403	25	.0501	.6203	.1427	1.38	1.41	.0595	.0384	.6719	.1287	1.56	1.62	.0835
.122	.403	.04	.0477	.6670	.1468	1.49	1.32	.0568	.0278	.7768	.1331	2.23	1.59	.0801
.600	.465	12	.0185	.8616	.1838	4.63	2.21	.0555	.0130	.8728	.1756	6.62	2.31	.0658
0	.465	12	.0512	.6498	.1526	1.38	1.39	.0783	.0487	.6463	.1474	1.42	1.42	.0875
.300	.570	12	.0258	.8408	.1792	3.17	1.82	.0778	.0194	.8592	.1849	4.81	1.92	.0677
.300	.360	12	.0780	.4873	.1494	1.05	1.04	.0336	.0463	.6354	.1326	1.35	1.36	.0624
.300	.465	17	.0340	.7683	.1512	2.41	1.33	.0879	.0177	.8249	.1370	4.21	1.81	.1128
.300	.465	5	.0294	.7307	.1433	2.44	2.09	.1030	.0197	.7967	.1475	3.84	2.17	.0957
.300	.465	12.5	.0361	.7409	.1530	2.16	1.55	.0803	.0231	.8103	.1479	3.14	1.71	.0890

10%, one can see that a large part of volume reduction is due to some other reasons. It is known that carbonation changes CSH gel to pure silica gel [6], and the oriented water molecules occupy more space than bulk water. Thus the loss of chemically combined water due to the carbonation results in shrinkage and is irreversable. With the exception of the mortar with F/(C+F)=0.60, the drying shrinkage recovered almost completely when RH > 97%, c.f. the adsorption of 2-I in Fig.4.

The water cured specimens (Series 2-II) had a higher moisture content at low RH than the standard cured specimens (Series 2-III). This might be due to the inadequate hydration and the carbonation of the surfaces of the mortar prisms of the latter during the RH 50% curing.

The change in the desorption isotherm due to carbonation also implies that a moisture gradient may exist in the concrete between the carbonated and non-carbonated zones even under the moisture equilibrium conditions. Microcracks are likely to occur in this type of zone.

The change in desorption isotherms reflects the pore system in the solid. Based on the isotherm, the distribution of pore size in the mortar can thus be calculated.

3.4 Relation between Desorption Isotherm and Mixture Proportions

The BET equation [2] can be used for calculating the specific surface area. But the calculation based on the data of this work shows no systematic relation between BET coefficient c and the properties of the material [8]. Therefore it cannot be used to generalize the feature of the isotherms. It has been found in this study that the desorption isotherm can be expressed by

$$W_e = \frac{W\infty}{1 + b\ \sqrt[s]{[\ln(p^\circ/p)]}} \qquad (4)$$

where W∞ is the moisture content of saturated mortar or total porosity. The deriva-tion of this formula is based on Halsey's equation [7] and given in [9]. Coefficient b is proportional to the ratio of total porosity to the specific surface area. s varies between 1 to 3, c.f. [7]. The coefficients b and s are obtained from the relation:

$$\frac{1}{W_e} = \frac{1+ b\ \sqrt[s]{[\ln(p^\circ/p)]}}{W_\infty} \qquad (5)$$

Plotting $1/W_e$ against $\sqrt[s]{\ln(p^\circ/p)}$, and trying different s values so that the linear regression gives $W_e(p^\circ/p=1)=W_\infty$. The specimens cured in water for 90 days have s value about 1, and s becomes larger when the specimens are carbonated. The b and s values calculated based on the experimental results are shown in Table 2. Eq (4) smooths the experimental data to a continuous curve and is valid for the mix proportion ranges tested in this study, see Fig.5. However, due to ignoring the pore size distribu-tion (see the deriving of eq (4) in ref.[9]) some abrupt change in the isotherm can not be fitted, e.g. the moisture loss between RH 33% and 42%.

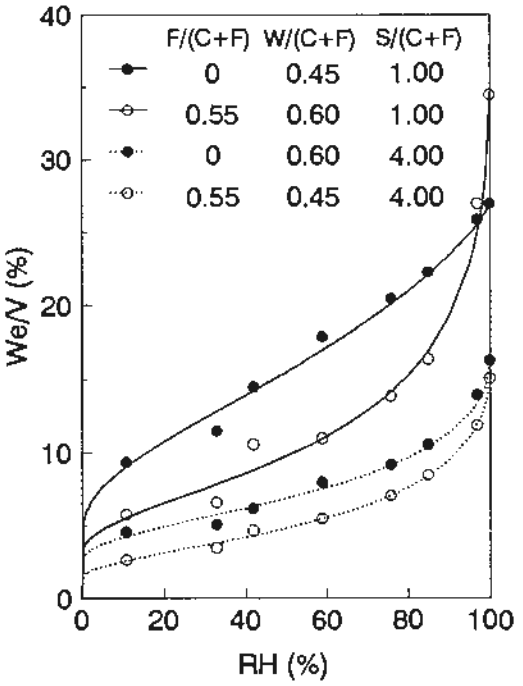

Fig.5 Desorption isotherms and curve fitting. Lines are drawn according to the regression by eq (5).

According to the derivation of eq (4), the value of the coefficient b should be proportional to the ratio of porosity to specific surface area, which is verified

by the relations shown in Fig.6.

The relations between the coefficients in eq (5) and the mixture proportions can be expressed empirically as

$$f = a_0 + \Sigma a_i X_i + \Sigma a_{ij} X_i X_j \quad (i,j=1,2,3) \qquad (6)$$

where f stands for a function of variables X_i (i=1,2,3), i.e.

$X_1=(F/(C+F)-0.300)/0.178$
$X_2=(W/(C+F)-0.465)/0.062$
$X_3=([CO_2]-12.48)/7.42.$

Analysing the data in Table 2 gives the coefficients a_i (i=1,2,3) well correlated with the mixture proportions as it is expressed by the F-test, Table 3. F_1 tests the lack of fitting and F_2 tests the fitting of the empirical formula. In this experiment, if $F_1 < 3.45$ and $F_2 > 4.94$ it means an insignificant lack of fitting and a very good correlation.

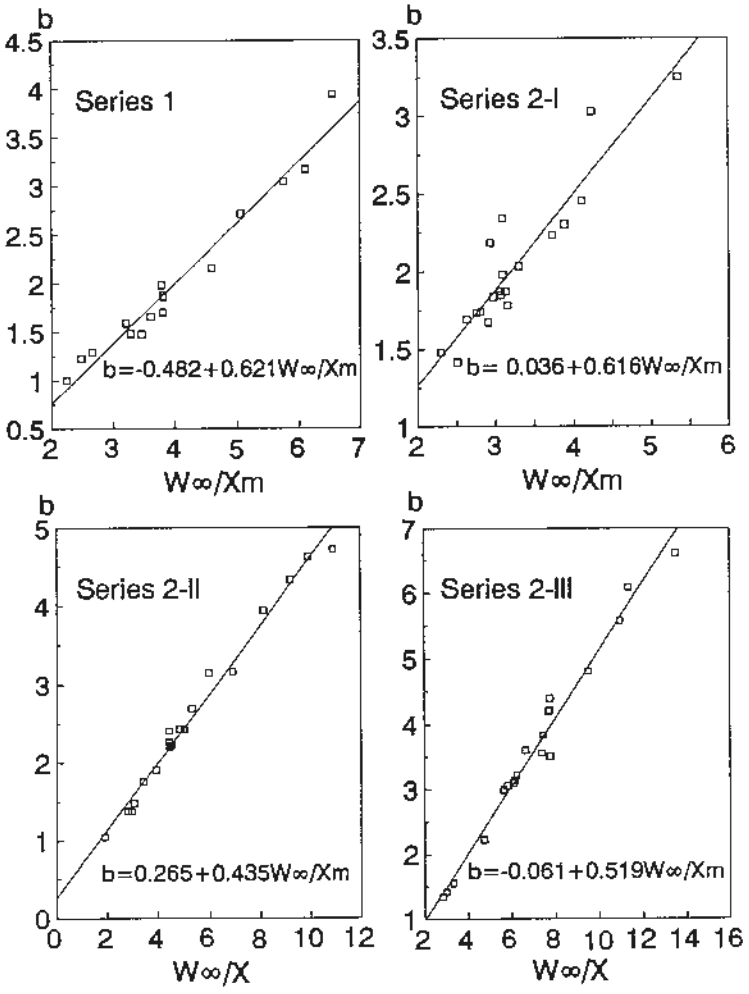

Fig.6 Relation between the porosity, specific surface area and the coefficient b in eq (4).

3.5 Pore Size Distribution

The moisture loss is due to the evaporation of water from two sources, i.e. from the walls of the emptied pores (film water) during drying, and from core of the capillaries with the average radius satisfying the Kelvin equation

$$r_m = r - t < \frac{-2\gamma V}{\ln(p/p^\circ)RT} \qquad (7)$$

where t is the thickness of the adsorbed water molecules layer.

As shown in Fig.2b, the moisture loss at RH > 59% increases due to the increase in fly ash content and water-to-binder ratio. The significant effect of these factors occurs at RH > 85%.

Table 3. Coefficients of empirical formulas (ref. eq.6) for describing the characteristics of the desorption isotherms of the carbonated cement mortar with PFA.

	Series 2-II						Series 2-III					
	Xm g/cm^3	K	W∞ g/cm^3	b	s	δW/V g/cm^3	Xm g/cm^3	K	W∞ g/cm^3	b	s	δW/V g/cm^3
a_0	.0361	.7409	.1530	2.1563	1.5470	.3507	.0231	.8103	.1479	3.4051	1.7107	.3487
a_1	-.0102	.0651	.0075	1.0093	.2508	.0115	-.0075	.0477	.0087	1.3652	.1529	.0109
a_2	-.0092	.0693	.0106	.5566	.1822	.0386	-.0052	.0466	.0151	.8563	.1610	.0381
a_3	.0013	-.0135	-.0006	-.1199	-.0091	.0065	.0008	-.0103	-.0017	-.0109	-.0311	.0061
a_{12}	.0030	-.0199	.0029	-.0164	.0427	-.0052	.0018	-.0142	.0007	.0283	-.0027	-.0051
a_{13}	.0002	-.0001	.0010	-.0472	-.0120	.0011	-.0011	.0102	.0010	.1322	.0094	.0004
a_{23}	.0000	.0015	.0010	.0042	.0051	.0031	-.0005	.0047	-.0001	.0437	-.0277	.0028
a_{11}	-.0004	.0057	.0056	.2970	.0847	.0034	.0028	-.0175	.0050	.1966	.0431	.0036
a_{22}	.0056	-.0267	.0042	-.0200	-.0474	.0007	.0035	-.0218	.0040	-.1356	-.0356	.0010
a_{33}	-.0038	.0189	-.0012	.2009	.0532	.0011	-.0024	.0116	-.0012	.1463	.0501	.0010
F_1	3.20	2.83	2.10	.56	7.61	.83	14.04	6.46	.68	3.81	8.15	.77
F_2	7.65	8.10	9.95	51.24	4.38	53.33	8.24	7.84	19.90	25.74	2.74	55.47

According to Kelvin's equation the core radii of the pores corresponding to RH 59% and 85% are 20 Å and 67 Å , i.e. small capillaries [4].

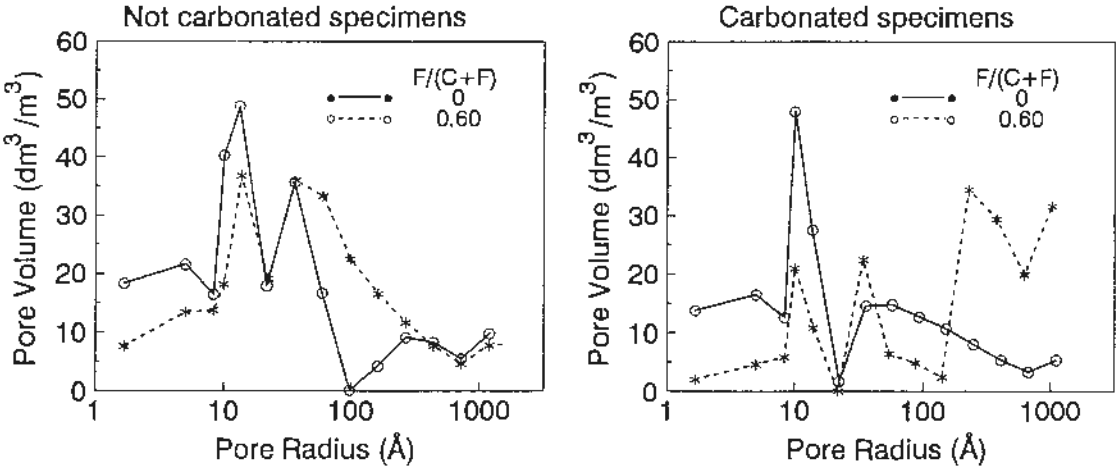

Fig.7 Pore size distribution according to desorption isotherms.

The pore size distribution analysis clearly shows that high fly ash content and carbonation lead to the coarser pore structure, Fig.7. The capillary pore size distribution is calculated according to Kelvin's equation and by taking into account the film water adsorbed at the inner surface of the capillary. The micro pore size distribution is estimated by the MP-method [10]. The pores are assumed to be slit shaped and the thickness of the film water is calculated by Halsey's equation [7,9].

The pore size distribution (Fig.7) follows a logarithmic normal distribution. There are two expectation values (mean value of the distribution) representing the gel pore and capillary pores. The large amount of fly ash addition and carbonation lead to the shifting of the average size of capillary pores to the right hand side, i.e. larger pore size direction.

4. CONCLUSIONS

The replacement of cement with fly ash changes the isotherms in two cases, i.e., (1) when the replacement fraction is higher than 30%, the pore system becomes coarser and results in a larger moisture loss at high relative humidity (e.g. RH > 90%), and (2) when the mortar is carbonated the increase in fly ash content leads to coarser pores in the mortar with a medium water to binder ratio. When F/(C+F) < 0.30 the specific surface area of the hardened paste increases slightly where fly ash exists which is mainly attributed to the hydration of fly ash, and the isotherm is only slightly affected.

The carbonated mortar has a lower total porosity but a coarser pore structure. The analysis indicates that the decomposition of CSH gel as well as the conversion of $Ca(HO)_2$ to $CaCO_3$ has taken place.

The sorption isotherms of cement mortar depend on the pore structure of the hardened cement paste, and reveal the specific surface area and the pore size distribution. The isotherms can be expressed by the function proposed in this paper, i.e.,

$$W_e = \frac{W\infty}{1 + b\sqrt[s]{[\ln(p^\circ/p)]}}$$

in which coefficients b and s characterize the isotherm determined in this work. b is proportional to the total porosity and inversely proportional to the specific surface area. The value s may be used in calculating the thickness of the adsorbed layer, but, further evaluation of its validity is necessary.

5. REFERENCES

/1/ ASTM E-104 85, "Standard Practice for Maintaining Constant Relative Humidity by Means of Aqueous Solutions", Annual Book of ASTM Standards. 14.02 (1988).

/2/ Stephen Brunauer, Jan Skalny, and E.E.Bodor, "Adsorption on Nonporous Solids", J. Colloid and Interface Science. Vol.30, No.4 pp 546 - 552 (1969).

/3/ S.J.Gregg and K.S.W.Sing, Adsorption, Surface Area and Porosity. Acadamic Press, (2nd edi.) (1982).

/4/ P.Kumar Mehta, Concrete Structure, Properties, and Materials. Prentice-Hall, Inc. Englewood Cliffs, (1986).

/5/ N.R.Draper and H.Smith, Applied Regression Analysis, (2nd edi.) (1981).

/6/ Kazutaka Suzuki, Tadahiro Nishikawa, Suketoshi Ito, "Formation and Carbonation of C-S-H in Water", Cement and Concrete Research. Vol 15, pp 213-224 (1985).

/7/ G. Halsey, "Physical Adsorption on Non-Uniform Surfaces", J of Chemical Physics, Vol 16 No 10 (1948).

/8/ Xu Aimin, "Sorption Isotherms of Cement Mortar Incorporating Fly Ash", Third CANMET/ACI Int. Conf. on Fly Ash, Silica Fume, Slag & Natural Pozzolans in Concrete, Trondheim, Norway, 1989. Supplementary Papers pp 173 - 187.

/9/ Xu Aimin, "The Structure and some Physical Properties of Cement Mortar with Fly Ash", Chalmers University of Technology, (to be published).

/10/ R.Sh.Mikhail, S.Brunauer, and E.E.Bodor, "Investigation of a Complete Pore Structure Analysis", J. Colloid and Interface Science Vol. 26, pp 45-53 (1968).

APPENDIX

Desorption data (kg/m^3) Series 2-I

$\frac{F}{C+F}$	$\frac{W}{C+F}$	Relative humidity (%)							
		11	33	42	59	76	85	97	100
.478	.527	34.3	44.2	69.6	92.3	129.4	163.9	204.2	219.8
.478	.403	33.5	44.4	71.7	94.6	127.7	156.2	181.8	189.9
.122	.527	45.7	55.3	80.7	106.2	139.9	171.3	197.0	216.1
.122	.403	43.5	54.3	80.4	102.2	133.9	152.6	164.0	178.7
.600	.465	31.5	37.3	56.9	77.9	112.6	145.0	196.9	215.1
0	.465	47.3	57.6	82.4	106.9	137.2	161.2	175.8	197.0
.300	.570	42.1	50.9	79.6	96.2	140.6	165.8	202.0	222.8
.300	.360	41.0	52.2	80.1	102.8	130.1	142.1	152.7	168.9
.300	.465	42.6	53.0	79.9	105.7	140.4	162.7	183.7	198.4

Desorption data (kg/m^3) Series 2-II

$\frac{F}{C+F}$	$\frac{W}{C+F}$	$[CO_2]$ (%)	Relative humidity (%)							
			11	33	42	59	76	85	97	100
.478	.527	25	25.4	33.6	40.9	41.1	50.6	62.8	110.1	185.5
.478	.527	.04	23.1	28.9	35.3	37.4	40.8	52.5	153.2	176.1
.478	.403	25	23.7	33.7	44.8	46.8	55.5	61.9	96.7	146.9
.478	.403	.04	21.5	30.0	37.6	40.9	48.0	56.5	134.7	184.0
.122	.527	25	33.5	43.7	58.0	64.4	77.8	83.7	121.8	157.8
.122	.527	.04	30.5	39.4	50.1	61.4	75.0	93.7	143.8	167.0
.122	.403	25	40.1	57.2	73.3	78.1	85.6	101.6	120.4	142.7
.122	.403	.04	39.6	52.6	69.4	77.0	91.1	105.5	133.3	146.8
.600	.465	12	25.4	28.1	37.1	38.4	50.4	62.6	104.9	183.2
0	.465	12	43.9	57.5	79.5	82.0	93.3	107.4	139.3	152.6
.300	.570	12	31.9	37.5	48.8	50.3	67.5	87.8	142.6	179.2
.300	.360	12	45.5	63.6	92.0	96.7	116.8	120.7	135.2	149.4
.300	.465	17	28.8	36.4	55.8	60.4	82.6	84.8	138.6	151.2
.300	.465	5	31.1	34.6	52.6	56.8	62.0	62.2	92.0	143.3
.300	.465	12.5	33.3	46.0	59.2	63.7	77.8	91.5	129.6	154.3

Desorption data (kg/m^3) Series 2-III

$\frac{F}{C+F}$	$\frac{W}{C+F}$	$[CO_2]$ (%)	Relative humidity (%)							
			11	33	42	59	76	85	97	100
.478	.527	25	17.2	23.7	32.1	32.3	40.3	49.8	82.4	179.2
.478	.527	.04	19.8	22.2	35.0	37.0	40.2	50.0	94.3	177.2
.478	.403	25	17.5	25.3	35.1	36.0	44.8	52.7	80.0	145.1
.478	.403	.04	18.6	28.1	35.7	37.8	47.1	55.1	93.6	149.5
.122	.527	25	25.4	35.9	45.8	46.9	57.8	68.4	104.0	153.1
.122	.527	.04	27.2	33.3	42.6	44.6	52.5	64.1	126.2	165.1
.122	.403	25	36.1	45.3	59.2	62.0	77.7	83.8	104.4	128.7
.122	.403	.04	28.7	37.6	47.8	51.0	64.7	74.9	118.6	133.1
.600	.465	12	16.2	21.0	27.8	28.1	34.1	43.0	78.6	174.4
0	.465	12	40.8	60.3	70.9	78.2	90.0	99.0	130.3	147.4
.300	.570	12	22.5	28.3	38.2	39.5	51.3	64.9	110.8	184.5
.300	.360	12	38.2	53.0	67.3	68.3	89.2	95.7	116.1	132.6
.300	.465	17	18.2	23.6	29.5	38.5	43.8	51.0	81.7	137.0
.300	.465	5	21.1	30.1	38.0	38.1	46.0	52.4	77.5	147.6
.300	.465	12.5	23.5	32.6	41.7	44.6	58.2	71.6	109.1	149.3